Supporting Information for:

Monoacylglycerols as Transmembrane Cl^- Anion Transporters

Soheila Bahmanjah, Ning Zhang and Jeffery T. Davis*

*Corresponding Author

Prof. Jeffery T. Davis

Department of Chemistry and Biochemistry, University of Maryland

College Park, MD 20742, USA

Phone: (001) 301-405-1845; e-mail: jdavis@umd.edu

Table of Contents

General Experimental. The ^{1}H NMR spectra were recorded on either a Bruker DRX-400 operating at 400.13 MHz, or a Bruker AVIII-600 operating at 600.13 MHz. All ^{13}C NMR spectra were recorded on a Bruker DRX-400 operating at 100.61 MHz. Chemical shifts are reported in ppm relative to the residual protonated solvent peak. ESI-MS experiments were done with a JEOL AccuTOF spectrometer. Chromatography was performed using 60-200 mesh silica gel from Baker. Thin layer chromatography was performed on Kieselgel 60 F254 silica-coated glass plates and visualized by UV and CAM stain. The pH of solutions was monitored with a Fisher Scientific AR25 dual channel pH/ion meter. Deuterated solvents were purchased from Cambridge Isotope Labs. Chemicals and solvents were purchased from Aldrich, Fisher, or Acros. Compounds **1a**, **1b**, **2** and **3** were purchased from commercial sources and used without any further purification. Phospholipids used to prepare liposomes were purchased from Avanti Polar Lipids. Liposome fluorimetric assays were recorded using a Hitachi F-4500 spectrophotometer. High-pressure extrusion was performed on the Avanti mini-extruder with a 0.1 μm polycarbonate membrane. Size-exclusion chromatography was performed using Sephadex G25.

Synthetic Procedures.

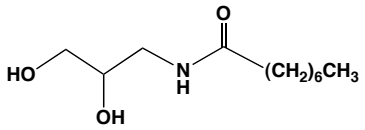

N-Octanoyl-(R,S)-3-amido-1,2-propanediol (4a). 3-Amino-1,2-propanediol (517 mg, 5.5 mmol) was dissolved in anhydrous DMF (5 mL) and cooled to 0 °C in an ice-bath, followed by consecutive additions of octanoyl chloride (862 µL, 5 mmol) and triethylamine (700 µL, 5 mmol). The ice-bath was removed after 10 min. The reaction mixture was left to stir overnight at rt. The DMF solution was diluted with ethyl acetate (75 mL) and transferred to a separatory funnel and washed with water (5 x 30 mL). The organic layer was dried over Na_2SO_4 and evaporated to give a white solid. The crude product was crystallized from hot MeOH to give a white product (0.51 g, 47% yield). ^{1}H-NMR (DMSO-d_6, 400.13 MHz, 25 ℃) δ: 7.75 (t, 1H, NH), 4.72 (d, J = 4.8 Hz, 1H, 2'-OH), 4.51 (t, J = 5.9 Hz, 1H, 1'-OH), 3.44 (m, 1H, 2'-CH), 3.26 (m, 2H, 1'-CH_2), 3.16 (m, 1H, CH-N), 2.96 (m, 1H, CH-N), 2.07 (t, J = 7.4 Hz, 2H, -CH_2-), 1.47 (m, 2H, -CH_2-), 1.23 (m, 8H, -$(CH_2)_4$-), 0.86 (t, J = 6.8 Hz, 3H, -CH_3). ^{13}C-NMR (DMSO-d_6, 100.61 MHz, 25 ℃) δ: 174.3, 71.6, 64.5, 63.8, 43.1, 36.3, 32.1, 29.5, 26.3, 23.0, 14.9. Mass Calculated: 217.17; ESI$^+$ Mass Found (M^+ + 1): 218.23.

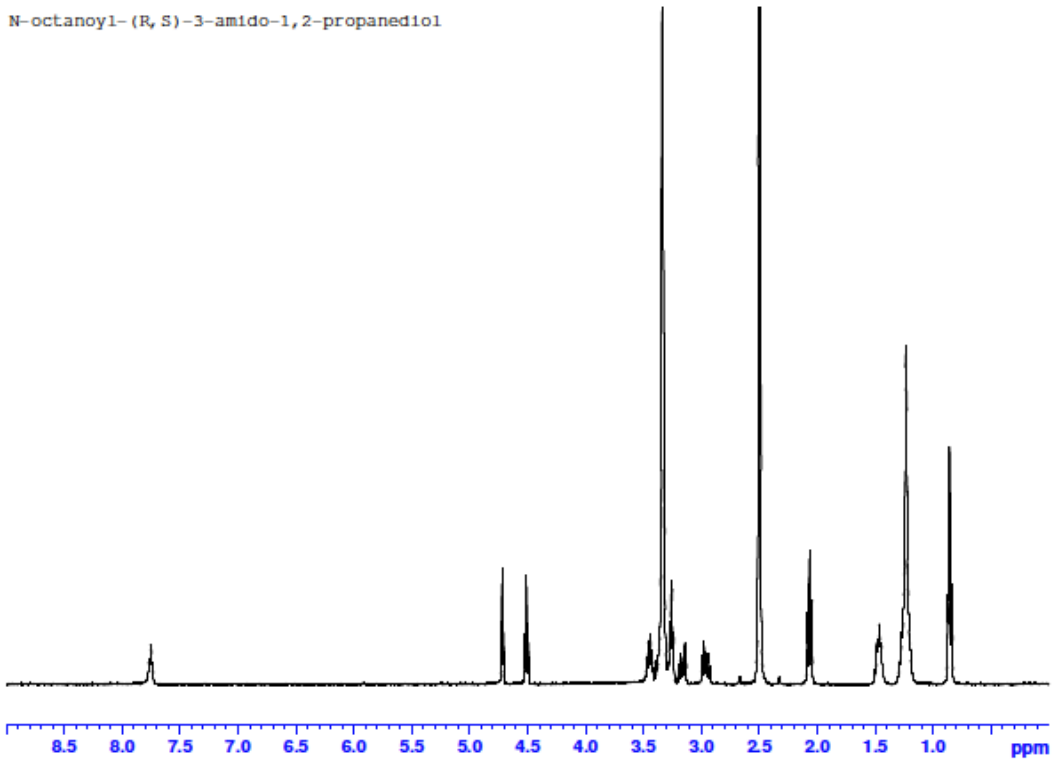

Figure S1. ^{1}H-NMR (400.13 MHz) spectrum of N-octanoyl-(R,S)-3-amido-1,2-propanediol **4a** in DMSO-d_6.

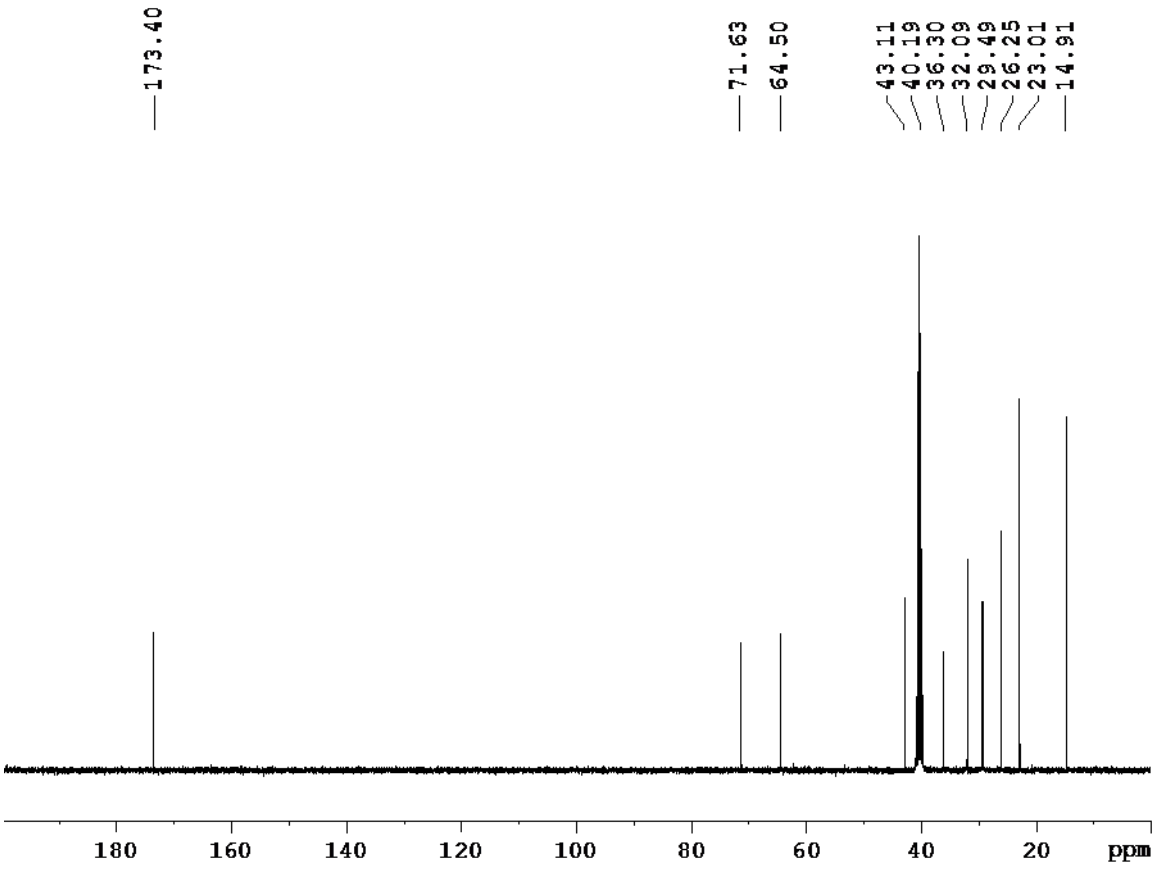

Figure S2. ^{13}C-NMR (100.61 MHz) spectrum of N-octanoyl-(R,S)-3-amido-1,2-propanediol **4a** in DMSO-d_6.

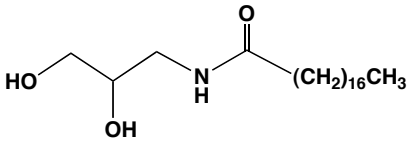

N-Stearoyl-(R,S)-3-amido-1,2-propanediol (4b). Stearoyl chloride (937 mg, 3 mmol) and 3-amino-1,2- propanediol (345 mg, 3.6 mmol) were mixed in a 6 mL glass vial and heated to form a solution before transferring to an oil bath. The reaction mixture was stirred for 15 min at 90 °C. Next, triethylamine (2.0 mL, 14.3 mmol) was added and the reaction mixture was heated at 90 °C for 30 min. The reaction mixture became a clear solution after addition of 3 mL of anhydrous methanol. The solution was kept at 65 °C for 45 min and then air-cooled to rt to give a white precipitate as the product. The crude product was filtered and washed with methanol. The product was further purified by crystallization from hot methanol and benzene solutions before being used in liposome assays. (0.69 g, 64% yield) ^{1}H-NMR (DMSO-d_6, 400.13 MHz, 25 ℃) δ: 7.74 (t, J = 5.2 Hz, 1H, NH), 4.70 (d, J = 4.8 Hz, 1H, 2'- OH), 4.50 (t, J = 5.8 Hz, 1H, 1'- OH), 3.44 (m, 1H, 2' - CH), 3.26 (m, 2H, 1' – CH_2), 3.16 (m, 1H, CH - N), 2.95 (m, 1H, CH - N), 2.06 (t, J = 7.4 Hz, 2H, – CH_2 –), 1.47 (m, 2H, – CH_2 –), 1.23 (m, 28H, – $(CH_2)_{14}$–), 0.85 (t, J = 6.6 Hz, 3H, – CH3). Mass Calculated: 357.32; ESI$^+$ Mass Found (M^+ + 1): 358.37.

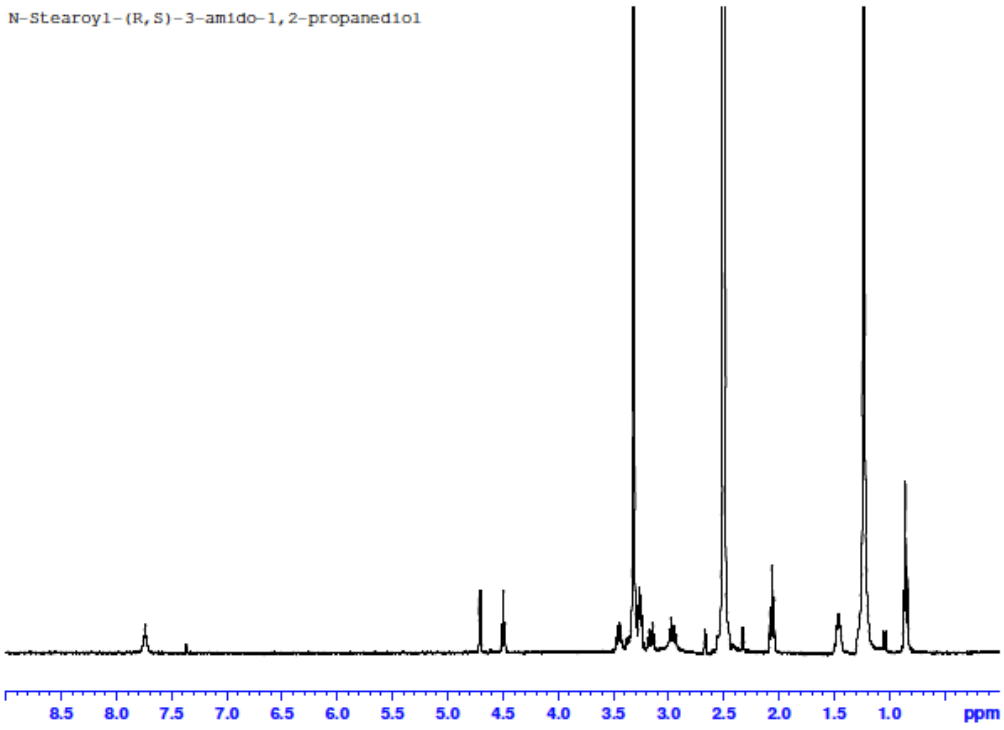

Figure S3. ^{1}H-NMR (400.13 MHz) spectrum of N-stearoyl-(R,S)-3-amido-1,2-propanediol **4b** in DMSO-d_6.

N-Perfluorooctanoyl-(R)-(+)-3-amino-1,2-propanediol (5). Methyl perfluorooctanoate (245 µL, 1.0 mmol) and (R)-3-amino-1,2-propanediol (192 mg, 2.0 mmol) were mixed in anhydrous methanol (5 mL) at room temperature. The reaction mixture was allowed to stir for 24 h at room temperature. Methanol was removed *in vacuo* and the crude product was re-dissolved in CH_2Cl_2:MeOH 5:1 and applied to a silica gel column and then eluted with CH_2Cl_2:MeOH 5:1. The appropriate fractions were collected, combined and evaporated to give a white solid (0.40 g, 82 % yield) R_f = 0.53 in CH_2Cl_2:MeOH 5:1. $[\alpha]_{20/D}$ +13.8° (methanol). ^{1}H-NMR (DMSO-d_6, 400.13 MHz, 25℃) δ: 9.39 (br s, 1H, NH), 4.86 (s, 1H, 2'- OH), 4.63 (br s, 1H, 1'- OH), 3.59 (m, 1H, 2' - CH), 3.30 (m, 3H, 1' – CH_2 & CH_2 - N, 3.13 (m, 1H, CH_2 - N). ^{13}C-NMR (DMSO-d_6, 100.61 MHz) δ: 157.2, 70.7, 64.8, 44.6. ^{19}F-NMR (DMSO-d_6, 376.12 MHz, 2,2,2-trifluoroethanol as reference) δ: -81.4 (t, J = 9.7 Hz, 3F, - CF_3), -119.6 (t, J = 12.5 Hz, 2F, CO - CF_2), -122.7 (br s, 2F, - CF_2 -), -123.1 (br s, 2F, - CF_2 -), -123.5 (m, 2F, - CF_2 -), -123.7 (br s, 2F, - CF_2 -), -127.0 (m, 2F, - CF_2 -). Mass Calculated: 487.03; ESI$^+$ Mass Found (M^+ +1): 487.99.

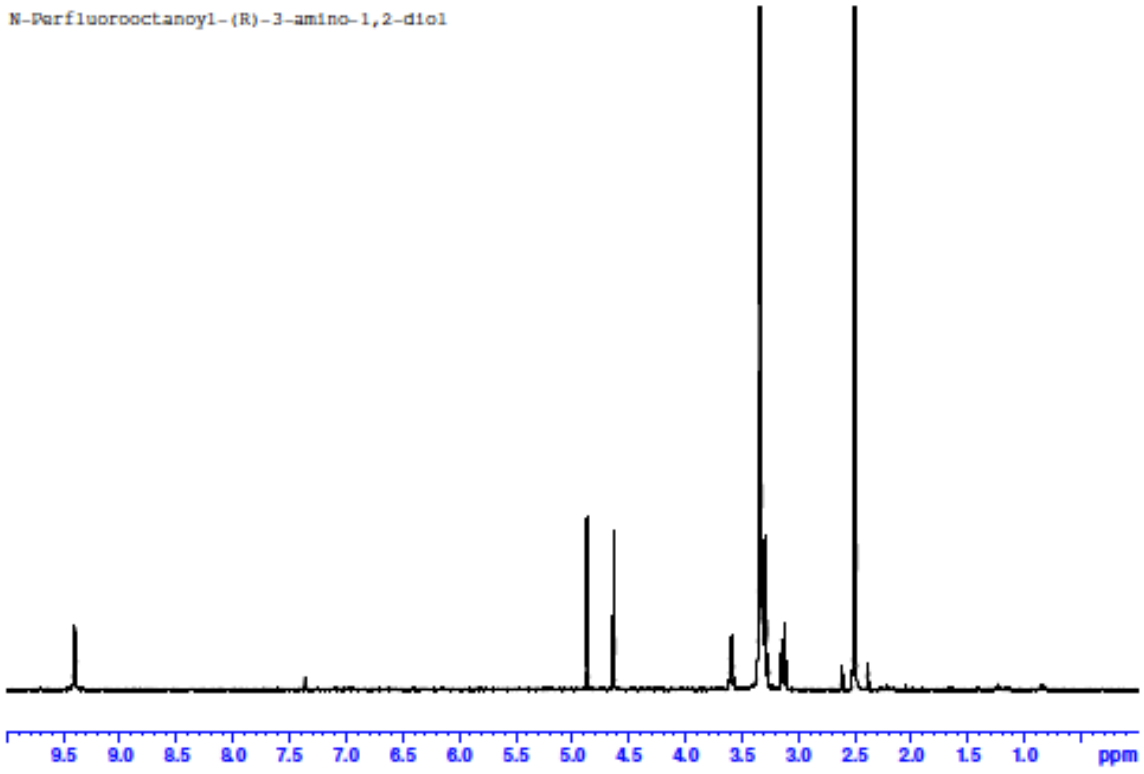

Figure S4. ^{1}H-NMR (400.13 MHz) spectrum of N-perfluorooctanoyl-(R)-(+)-3-amino-1,2-propanediol **5** in DMSO-d_6.

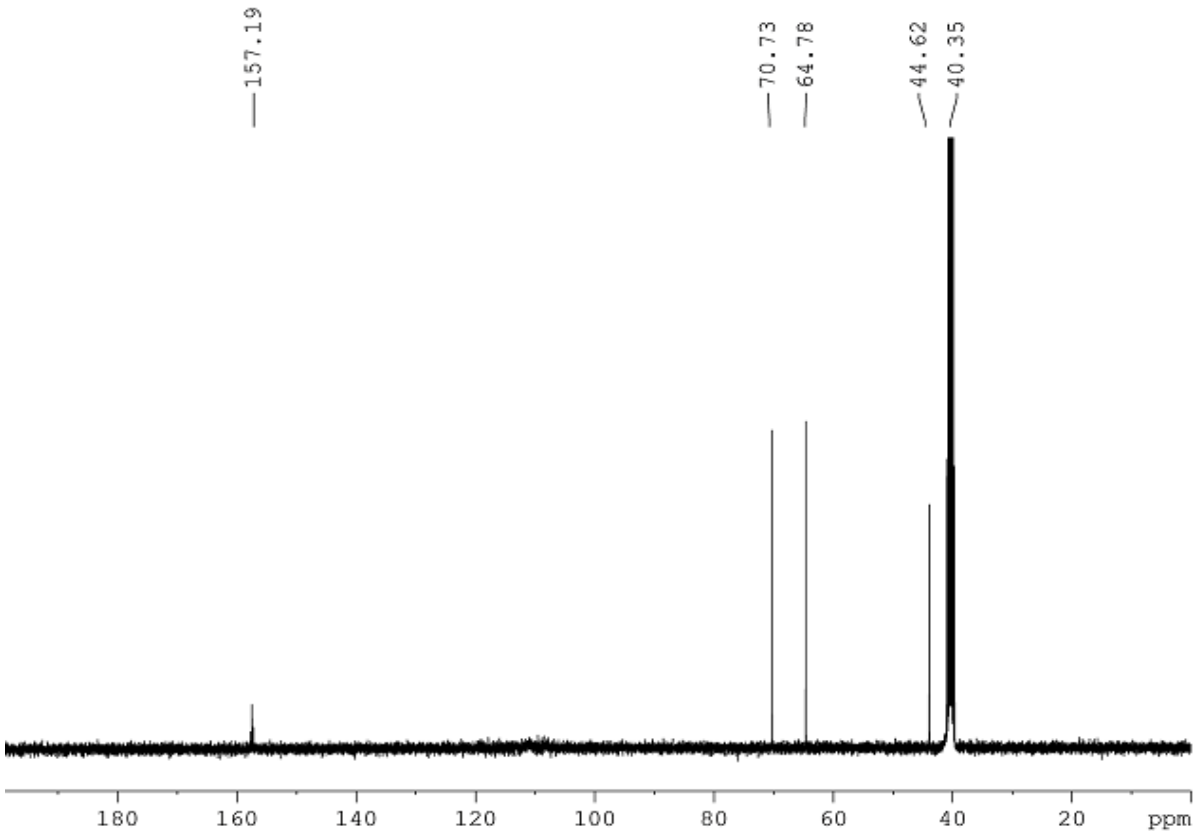

Figure S5. ^{13}C-NMR (100.61 MHz) spectrum N-perfluorooctanoyl-(R)-(+)-3-amino-1,2-propanediol **5** in DMSO-d_6.

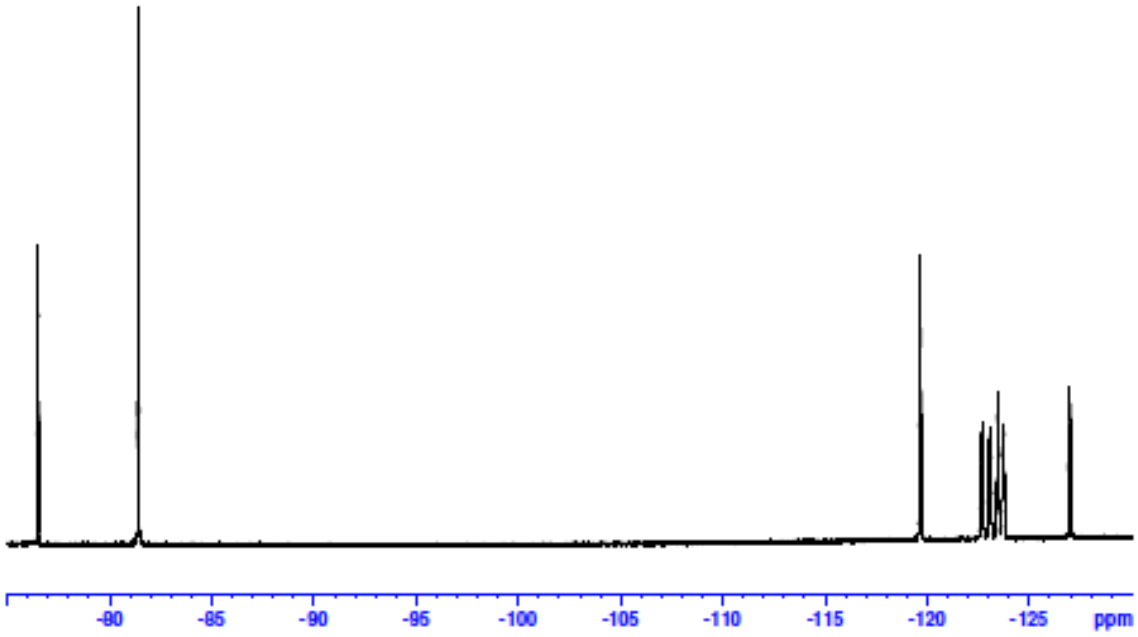

Figure S6. ^{19}F-NMR (376.12 MHz) spectrum of N-perfluorooctanoyl-(R)-(+)-3-amino-1,2-propanediol **5** in DMSO-d_6 (used 2,2,2-trifluoroethanol as reference).

N-Tetradecanoyl-(R)-(+)-3-amino-1,2-propanediol [(R-6)]. (R)-3-amino 1,2-propanediol (501 mg, 5.2 mmol) was dissolved in anhydrous methanol (6.5 mL) and the solution was cooled to -78 °C in an acetone-dry ice bath, followed by consecutive additions of myristoyl chloride (1,407 µL, 5 mmol) and triethylamine (800 µL, 5.7 mmol). The reaction mixture was allowed to stir overnight at room temperature. Next, anhydrous methanol (12 mL) was added and the reaction mixture was heated to give a solution. It was filtered and allowed to cool to room temperature. The pure product that precipitated from solution was collected and dried over vacuum. (0.63 g, 42 % yield) ^{1}H-NMR (DMSO-d_6, 400.13 MHz, 25 ℃) δ: 7.74 (t, J = 5.5 Hz, 1H, NH), 4.71 (d, J = 4.8 Hz, 1H, 2'- OH), 4.50 (t, J = 5.9 Hz, 1H, 1'- OH), 3.45 (m, 1H, 2' - CH), 3.26 (m, 2H, 1' – CH_2), 3.16 (m, 1H, CH - N), 2.96 (m, 1H, CH - N) 2.06 (t, J = 7.4 Hz, 2H, – CH_2 –), 1.46 (m, 2H, – CH_2 –), 1.23 (m, 20H, – $(CH_2)_{10}$–), 0.85 (t, J = 6.8 Hz, 3H, – CH_3). $[\alpha]_{20/D}$ + 6.8° (methanol). Mass Calculated: 301.26; ESI$^+$ Mass Found (M^+ + 1): 302.30.

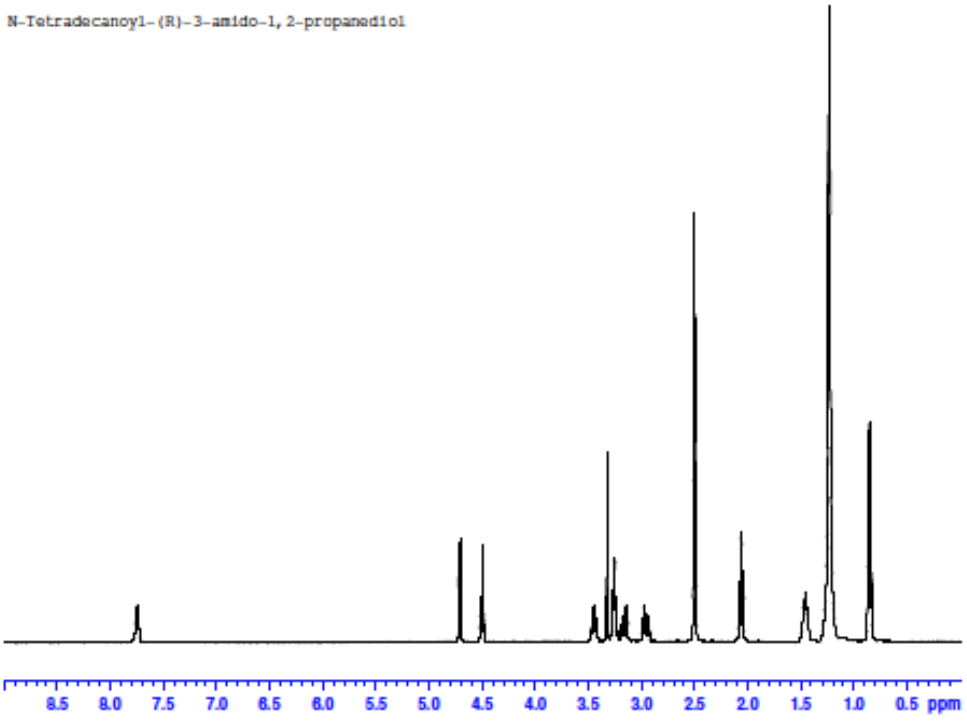

Figure S7. ^{1}H-NMR (400.13 MHz) spectrum of N-tetradecanoyl-(R)-(+)-3-amino-1,2-propanediol **(R)-6** in DMSO-d_6.

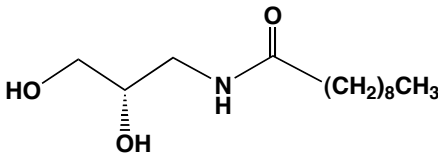

N-Tetradecanoyl-(S)-(–)-3-amino-1,2-propanediol [(S)-6]. Refer to procedure for synthesis of **(R)-6**. (0.65 g, 36 % yield) ^{1}H-NMR (DMSO-d$_6$, 400.13 MHz, 25 ℃) δ: 7.74 (t, J = 5.5 Hz, 1H, NH), 4.71 (d, J = 4.8 Hz, 1H, 2'- OH), 4.50 (t, J = 5.9 Hz, 1H, 1'- OH), 3.45 (m, 1H, 2' - CH), 3.26 (m, 2H, 1' – CH2), 3.16 (m, 1H, CH - N), 2.96 (m, 1H, CH - N), 2.06 (t, J = 7.4 Hz, 2H, – CH2 –), 1.46 (m, 2H, – CH2 –), 1.23 (m, 20H, – (CH2)10–), 0.85 (t, J = 6.8 Hz, 3H, – CH3). $[\alpha]_{20/D}$ –5.8° (methanol). Mass Calculated: 301.26; ESI$^+$ Mass Found (M^+ + 1): 302.30.

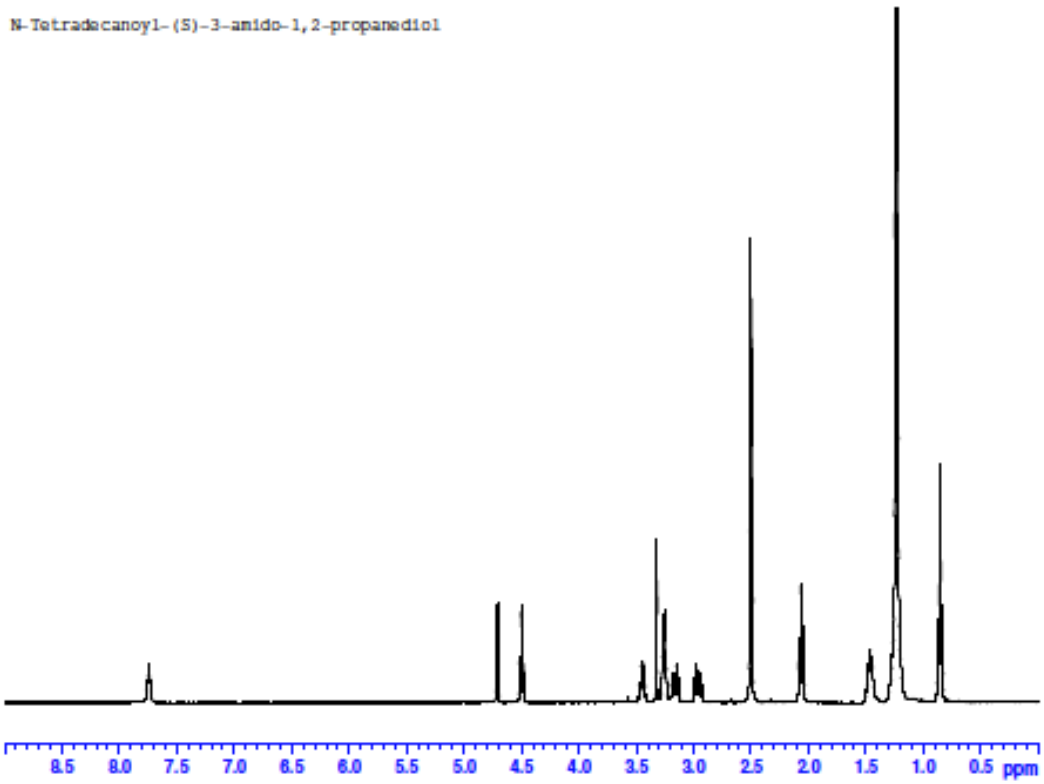

Figure S8. ^{1}H-NMR (400.13 MHz) spectrum of N-tetradecanoyl-(S)-(–)-3-amino-1,2-propanediol **(S)-6** in DMSO-d$_6$.

Preparation of Liposomes with Pre-Incorporated Transporter. Egg yolk phosphatidylcholine (EYPC) lipid (7.7 mg, 0.01 mmol) was dissolved in 10 mL of chloroform. The anion transporter (compounds **1-5**) was dissolved in methanol and a specific amount of the transporter stock solution was added to the EYPC solution to give a specific transporter:lipid ratio. The resulting EYPC-transporter solution was then evaporated under reduced pressure to produce a thin film that was dried in vacuum for 3 h. The lipid film was then hydrated with 1 mL of a solution containing HEPES buffer (20 mM), sodium nitrate (225 mM) and lucigenin dye (1 mM).[1] Using 5 mL of a 1M NaOH solution, the pH was adjusted to 7.4. A series of freeze/thaw cycles were repeated at least 9 times or until no solids were visible in solution. The frozen solution was warmed to 30-35 ^{o}C before each freeze cycle. The mixture was placed on a vortexer every 3 cycles for 30 s to facilitate hydration. Sizing of the resulting suspension to convert any large multi-lamellar vesicles (LMVs) to small unilamellar vesicles (SUV) was achieved using a standard extrusion process in which the suspension was passed through a 100 nm pore size polycarbonate filter up to 33 times at room temperature. To remove non-encapsulated dye in solution we used size exclusion chromatography. The liposome solution was loaded onto a Sephadex G-25 column (18 cm x 1.5 cm). The eluant contained HEPES buffer (20 mM, pH 7.4) and sodium nitrate (225 mM). Using a hand-held UV lamp the liposomes were visualized and isolated from any free dye. The eluted vesicles were diluted with aqueous $NaNO_3$ (225 mM) to give a final volume of 25 mL (0.4 mM in EYPC lipid). The size of the liposomes was confirmed by dynamic light scattering experiments (see p. S32).

Anion Transport Assays. This procedure describes a typical ion transport assay, as depicted in Figure 1 of the paper. An aliquot of the liposome suspension (3 mL) was placed in a cuvette at 25 ^{o}C, The fluorescence of the intravesicular lucigenin was monitored by excitation at 372 nm, and the emission was recorded at 503 nm with a 2.5 nm slit width.[1] At t = 30 s, a 870 µL aliquot of a 1 M NaCl stock was injected to give a final NaCl concentration of 225 mM at 25 ºC. At the end of the experiment, 10 % aqueous Triton-X was injected to lyze the liposomes.

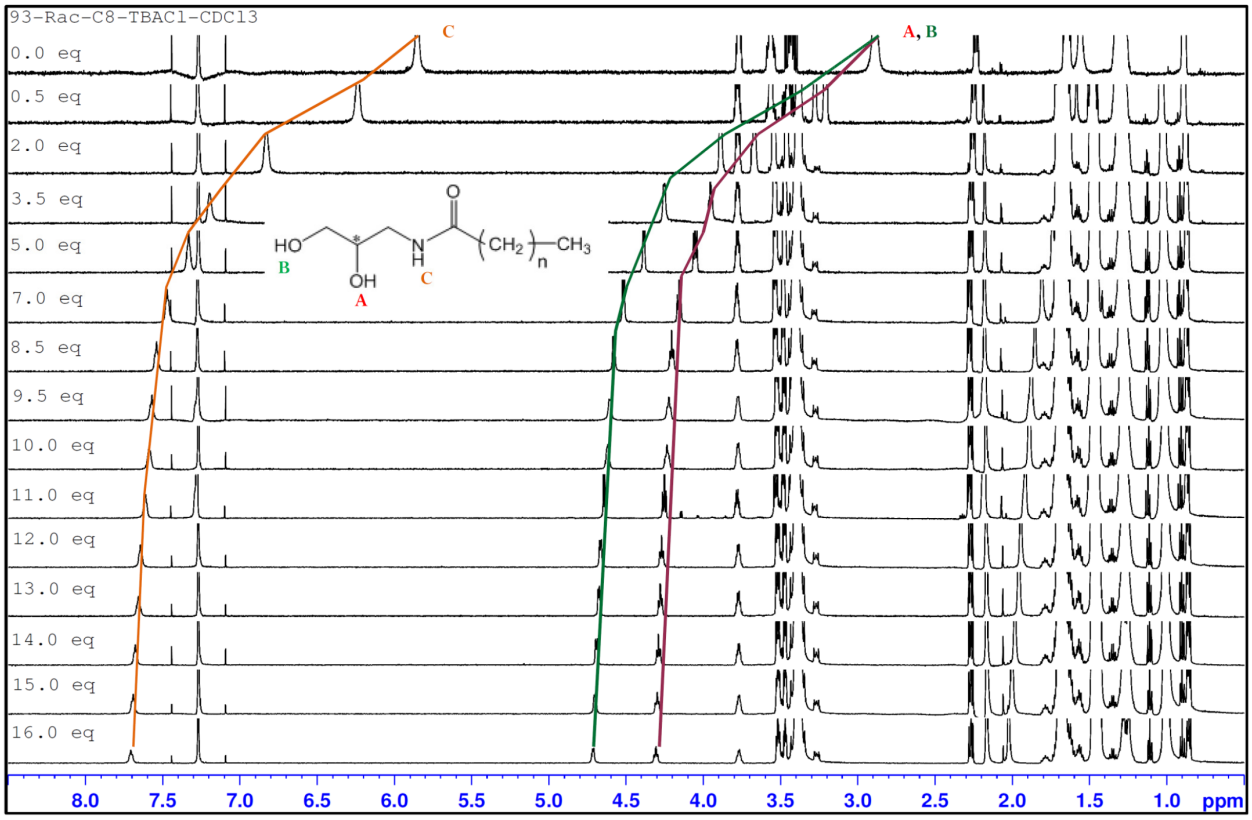

Figure S9. ^{1}H-NMR (600.13 MHz) stack plot of the amide **4a** (6 mM) with tetrabutylammonium chloride (TBACl) in $CDCl_3$. Addition of TBACl results in a downfield shifting of the NH and OH protons peaks. Changes in chemical shifts of the NH and OH protons for amide **4a** upon addition of anion confirmed that the head group of the compound is a potent anion binder. In $CDCl_3$ the two OH resonances for **4a** appeared together as a broad signal. The ^{1}H-NMR signals for the two different OHs were separated after addition of chloride anion. Addition of TBACl to the solution of **4a** in $CDCl_3$ resulted in large downfield shift for the NH ($\Delta\delta$ = 2.91) and OH signals ($\Delta\delta$ = 2.39 and 2.82 for the 1° and 2° -OH, respectively), consistent with formation of hydrogen bonds between chloride and these 3 acidic hydrogen atoms.

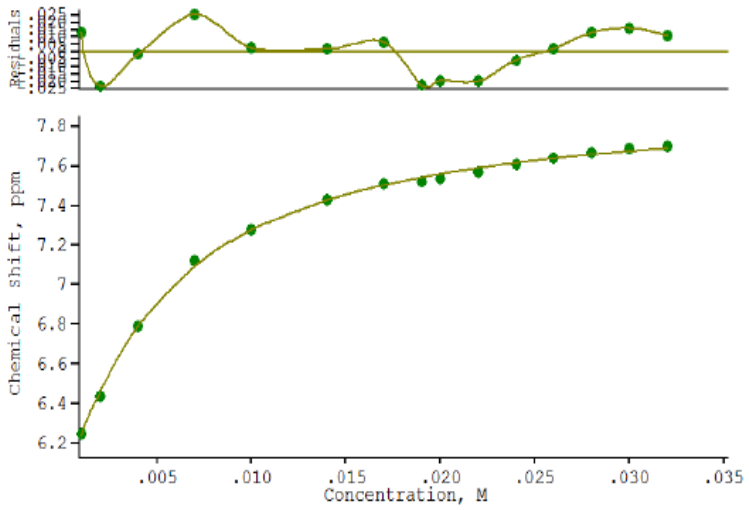

Figure S10. By evaluating chemical shift changes for the NH protons of amide **4a** (6 mM) during titration with TBACl in $CDCl_3$, we determined a binding constant of $K_a = 1474 \pm 32\ M^{-1}$ for amide **4a** and chloride. Compound **4a** with an amide NH linker binds chloride anion better than ester **1a** (see Fig. S13).

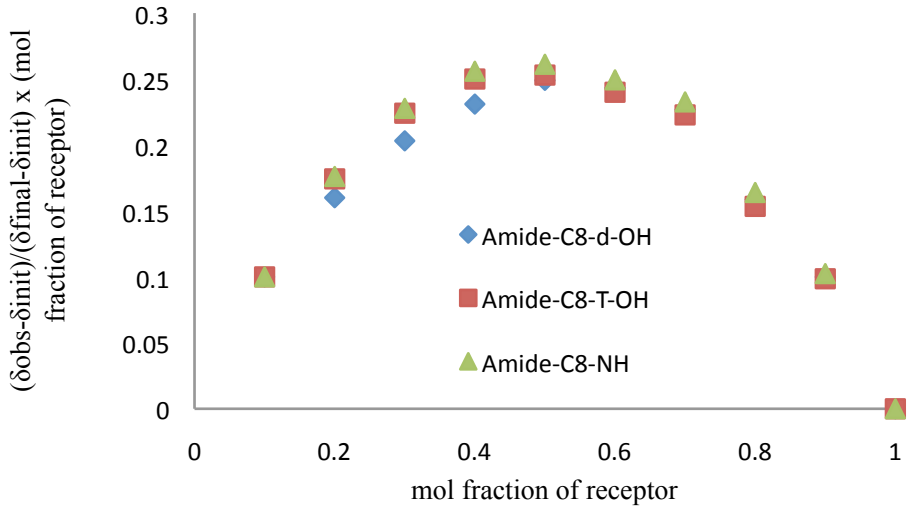

Figure S11. To determine the stoichiometry of the receptor-anion complex a Job plot was used. In this method, the total molar concentration of the compound and the anion are held constant but their molar fraction is varied. The observable variable that is proportional to complex formation (^{1}H-NMR chemical shift) is plotted against the mole fraction of the two components. The maximum of the plot correspond to the stoichiometry of the complex formed by two species. For amide **4a** the change in chemical shift of the exchangeable protons (NH and OH) of receptor molecule involved in binding chloride was plotted against the mole fraction of the receptor. The Job plots indicate that the amide **4a** forms a 1:1 complex with chloride anion.

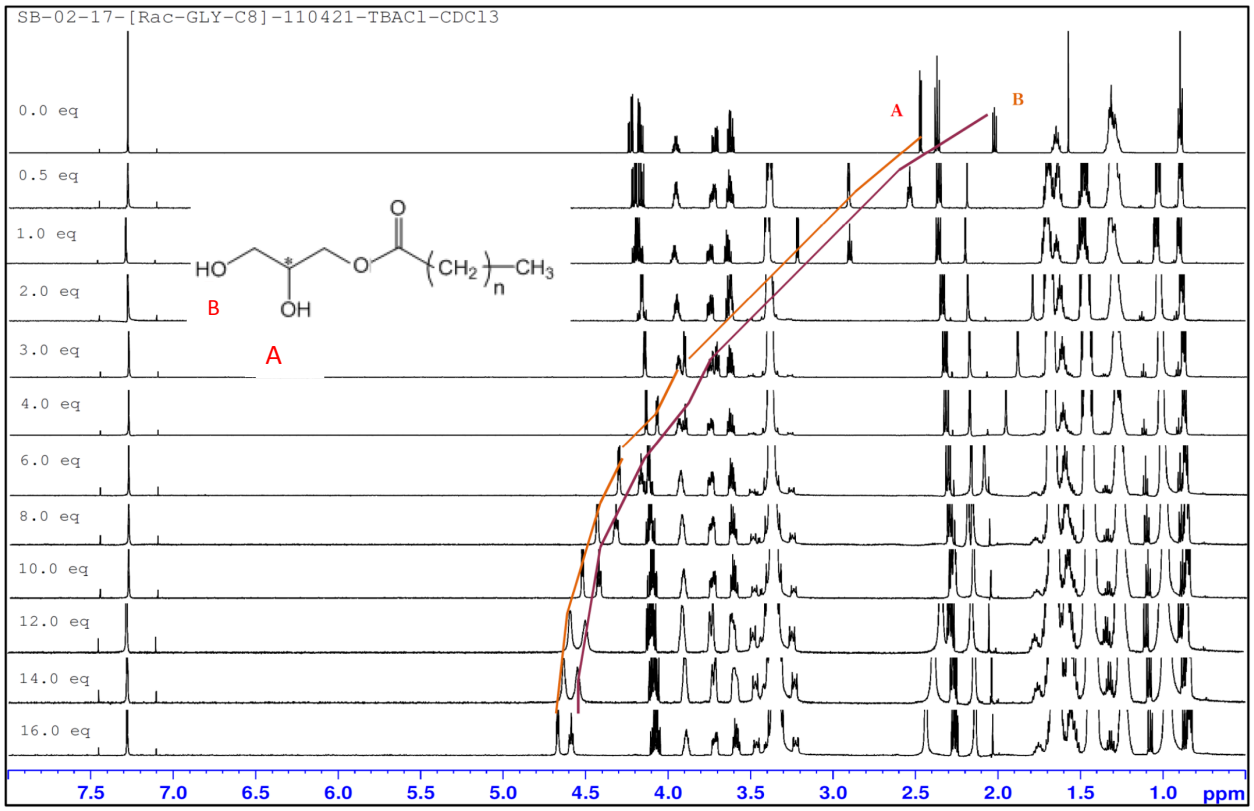

Figure S12. ^{1}H-NMR (600.13 MHz) stack plot of the compound **1a** (6 mM) with TBACl in $CDCl_3$. Addition of TBACl results in shifting of the peak for OH protons. Changes in chemical shifts of the OH protons for ester **1a** upon addition of anion demonstrate that the head group of the compound is a potent anion binder. In $CDCl_3$ the two OH resonances for **1a** appeared at 1.95 ppm and 2.56 ppm. Importantly, the ^{1}H-NMR signals for the two different OHs were shifted after addition of chloride anion. Addition of TBACl to the solution of **1a** in $CDCl_3$ resulted in large downfield shift for the OH signals ($\Delta\delta$ = 2.53 and 2.21 for the 2° and 1° -OH, respectively), consistent with formation of hydrogen bonds between chloride and these 2 acidic hydrogen atoms.

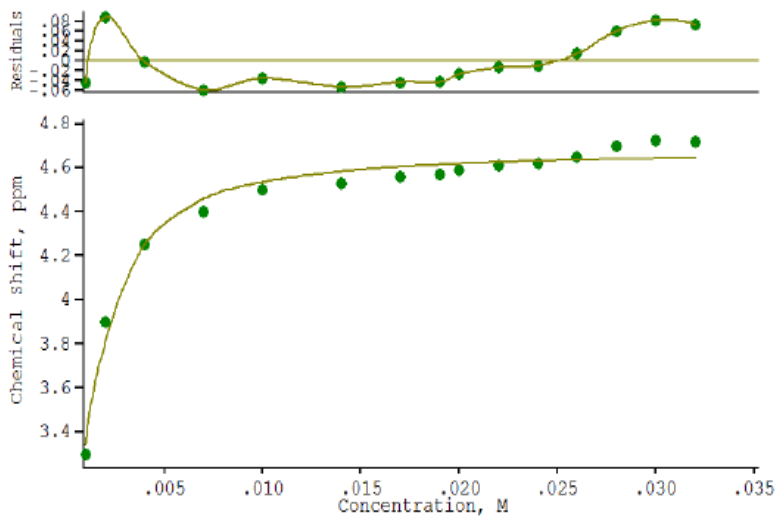

Figure S13. By evaluating chemical shift changes for the 1°-OH proton in ester **1a** (6 mM), during titration with TBACl in $CDCl_3$, we determined a binding constant of $K_a = 92 \pm 1.7\ M^{-1}$ for chloride and the primary hydroxyl group of ester **1a**.

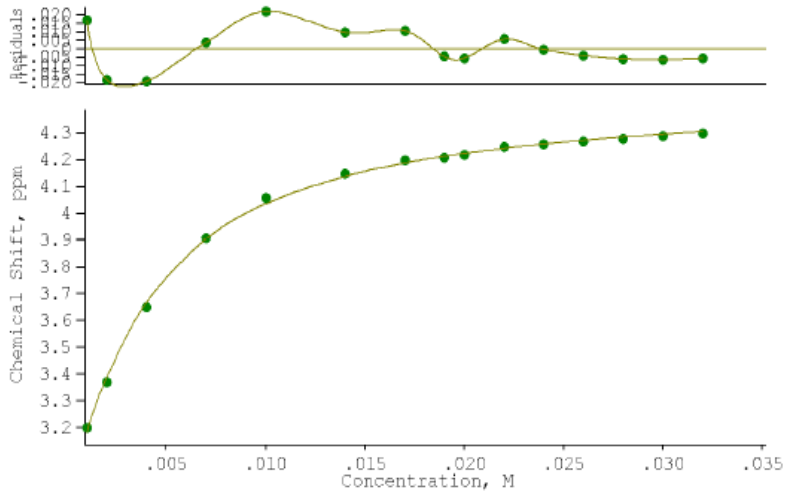

Figure S14. By evaluating chemical shift changes for the 2°-OH proton in ester **1a** (6 mM), during titration with TBACl in $CDCl_3$, we determined a binding constant of $K_a = 83 \pm 1.3\ M^{-1}$ for chloride and the secondary hydroxyl group of ester **1a**. Based on the comparative binding constants it is clear that amide **4a** with an amide NH linker binds chloride more strongly than does ester **1a**.

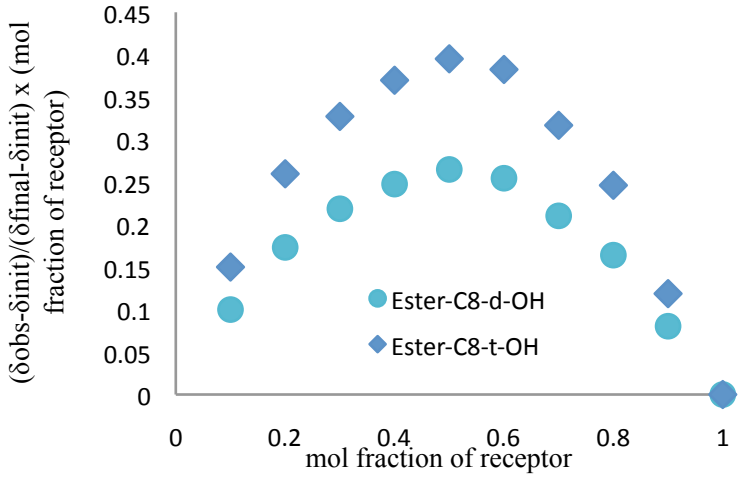

Figure S15. For ester **1a** the change in chemical shift of the exchangeable protons (OH) of receptor molecule involved in binding chloride was plotted against the mole fraction of the receptor. The Job plot indicates that the ester **1a** forms a 1:1 complex with chloride anion.

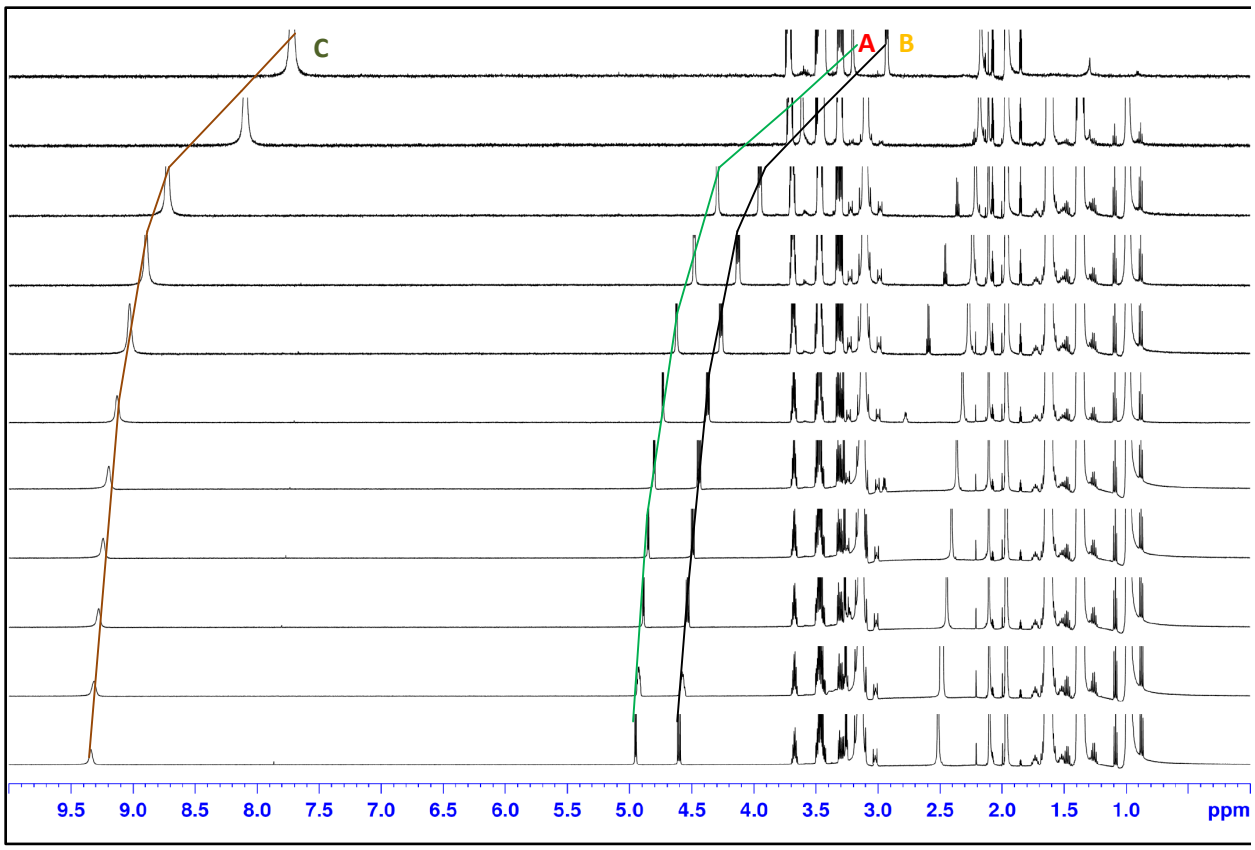

Figure S16. ^{1}H-NMR (600.13 MHz) stack plot of the fluorinated compound **5** (6 mM) with TBACl in CD_3CN. Addition of TBACl results in shifting of the peaks for the OH and NH protons. Changes in chemical shifts of the OH protons for fluorinated amide **5** upon addition of anion confirmed that the head-group of the compound is a potent anion binder. In CD_3CN the two OH resonances for **5** appeared at 3.11 ppm. Importantly, the ^{1}H-NMR signals for the two different OHs and NH were shifted after addition of chloride anion.

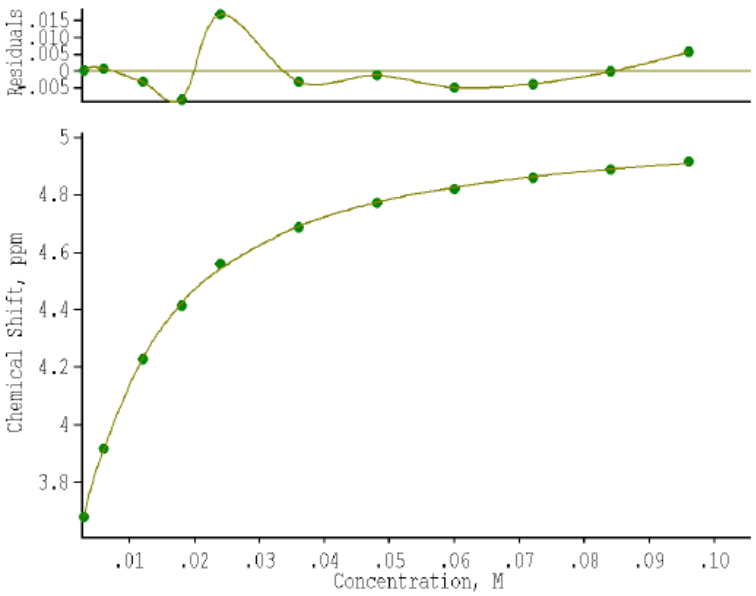

Figure S17. By evaluating chemical shift changes for the OH protons of fluorinated amide **5** (6 mM) during titration with TBACl in CD_3CN, we determined a binding constant of $K_a = 186 \pm 5.4\ M^{-1}$ for **5**.

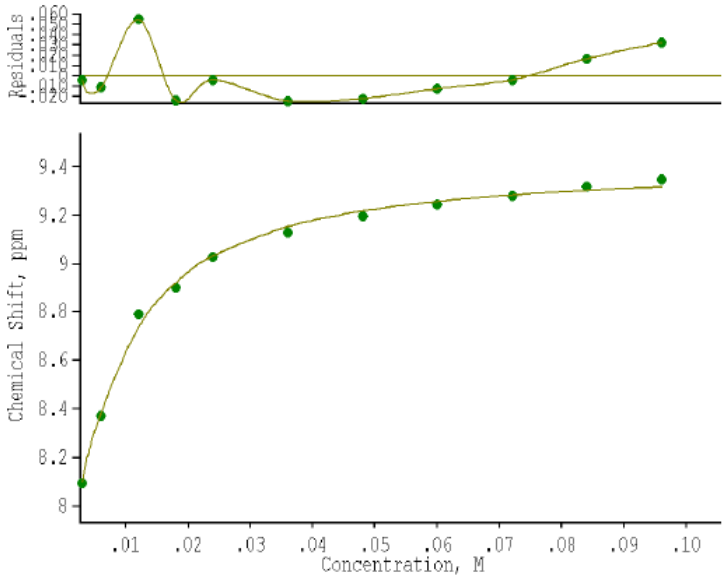

Figure S18. By evaluating chemical shift changes for the NH protons of fluorinated amide **5** (6 mM) during titration with TBACl in CD_3CN, we determined a binding constant of $K_a = 193 \pm 7.6\ M^{-1}$ for **5** NH group and chloride.

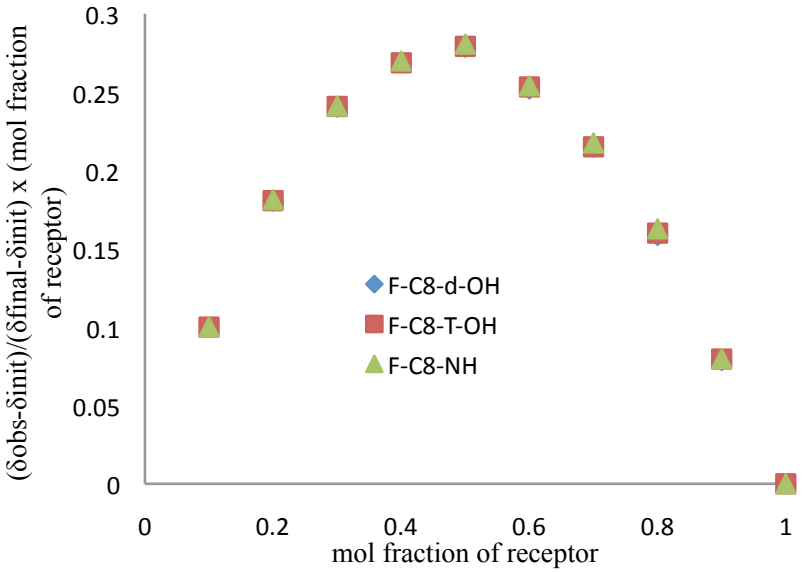

Figure S19. For fluorinated **5** the change in chemical shift of the exchangeable protons (NH and OH) of receptor molecule involved in binding chloride was plotted against the mole fraction of the receptor. The Job plots indicate that compound **5** forms a 1:1 complex with chloride anion.

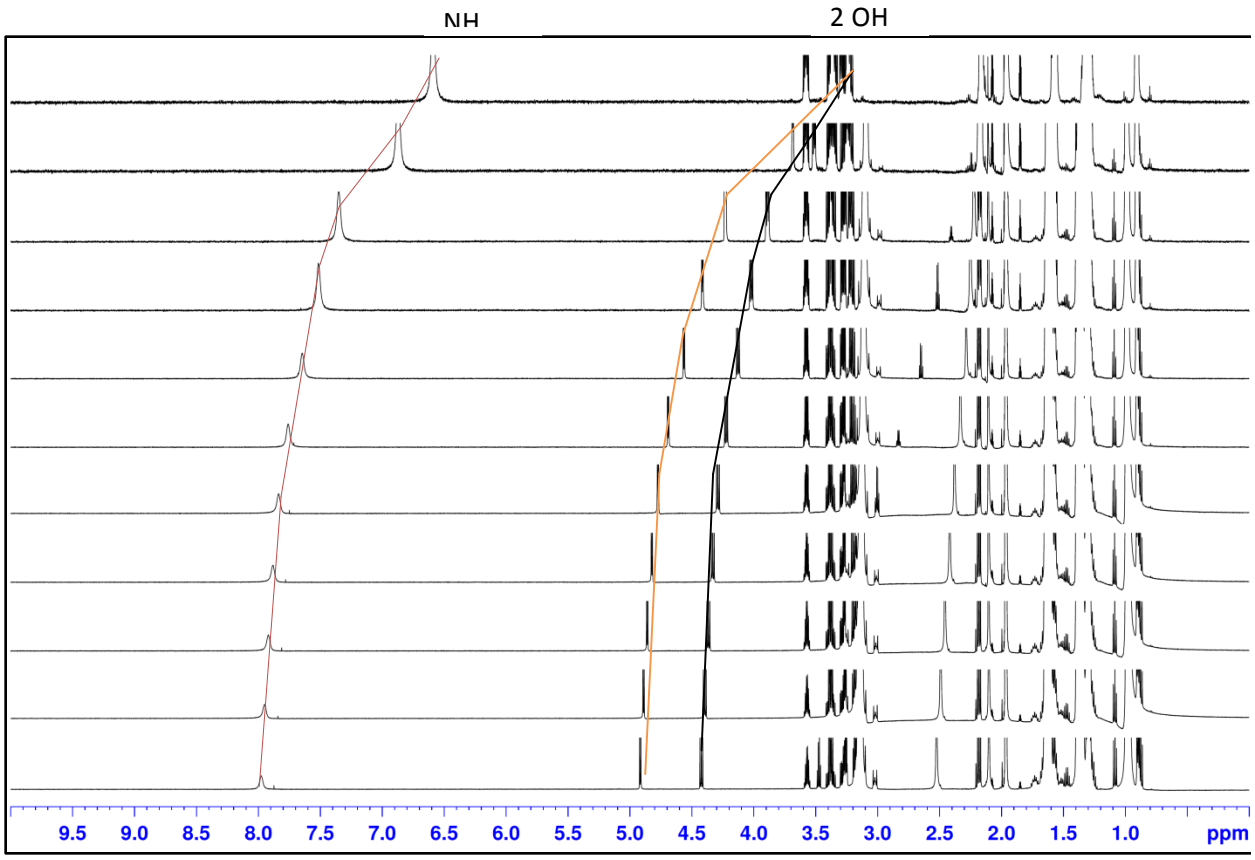

Figure S20. ^{1}H-NMR (600.13 MHz) stack plot of amide **4a** (6 mM) with TBACl in CD_3CN. Addition of TBACl results in downfield shift of the OH and NH protons signals. Changes in chemical shifts of the OH protons for amide **4a** upon addition of anion confirmed that the head group of the compound is a potent anion binder. In CD_3CN, the two OH resonances for **4a** appeared at 2.8 ppm and 3.11 ppm. Importantly, the ^{1}H-NMR signals for the two different OHs and NH were shifted after addition of chloride anion.

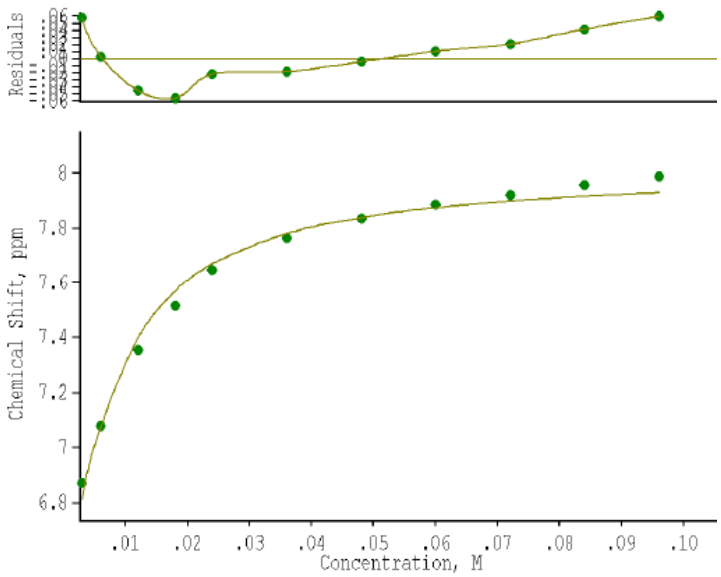

Figure S21. By evaluating chemical shift changes for the NH proton of amide **4a** (6 mM) during titration with TBACl in CD_3CN, we determined a binding constant of $K_a = 137 \pm 1.8\ M^{-1}$ for **4a** and chloride. The lower binding constant of **4a** vs. **5** shows that fluorinated amide **5** is a better chloride anion binder than amide **4a**.

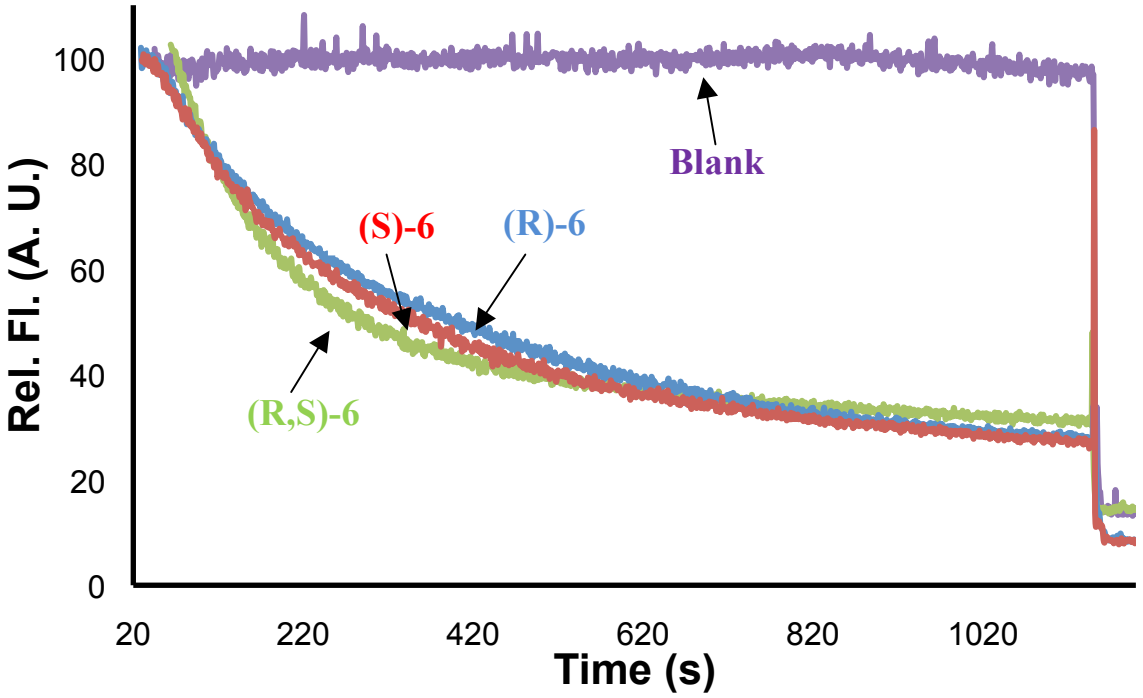

Figure S22. To determine if the stereochemistry of the amide's polar head group influences the efficiency of transmembrane anion transport, the (R) and (S) enantiomers of amide **6** were studied. Shown above are traces for Cl^- influx promoted by either 1 mol % of pre-incorporated (R)-**6**, (S)-**6** or (R,S)-**6** into unilamellar EYPC vesicles loaded with 225 mM $NaNO_3$, 20 mM HEPES buffer, pH 7.4. At the end of the experiment, detergent was added to lyse the vesicles and calibrate 100% chloride influx. There does not appear to be a significant difference between the transport properties for the (R)-**6** and (S)-**6** enantiomers.

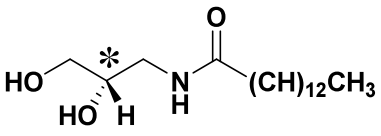

(S)-6

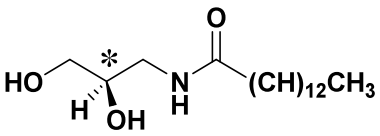

(R)-6

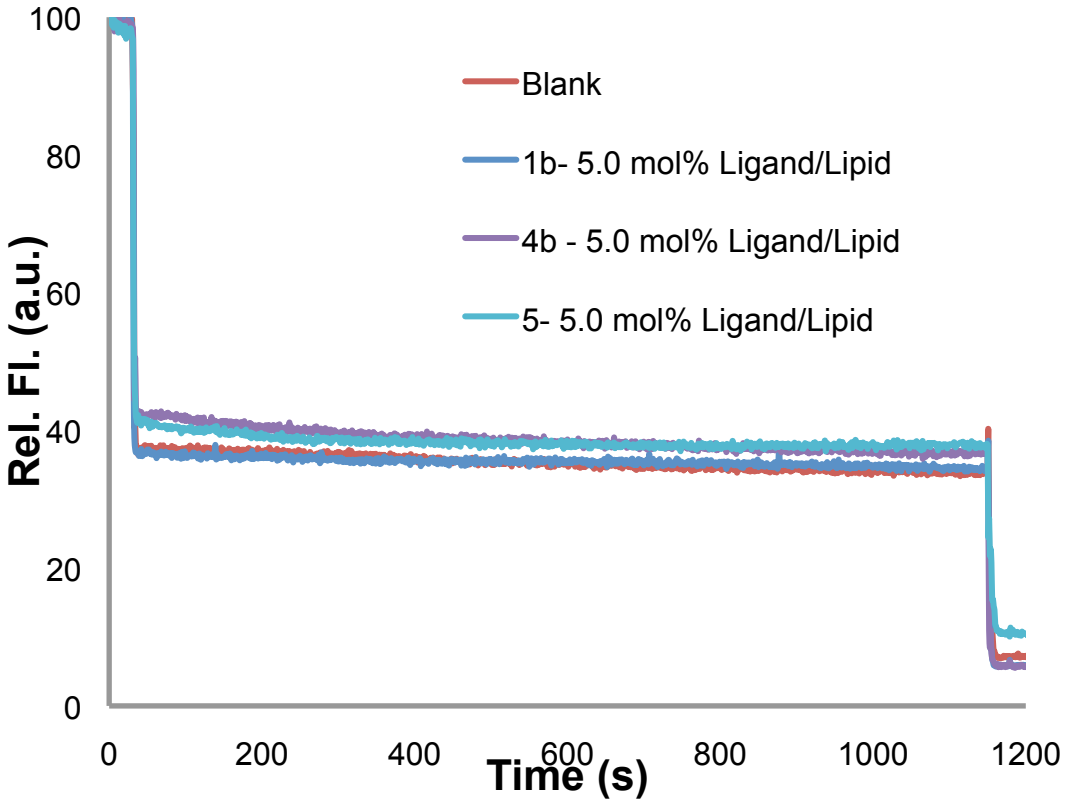

Figure S23. Chloride influx in the presence of 5 mol % of compounds **1b**, **4b**, and **5** into unilamellar EYPC vesicles loaded with 225 mM Na_2SO_4 buffered to pH 7.4 with 20 mM HEPES buffer. This experiment was performed to gain insight into the mechanism of transport. After addition of NaCl (225 mM) to EYPC liposomes containing 5 mol% of **1b**, **4b** or **5** (pH 7.4) we saw no Cl^- influx above background. Sulfate has a higher dehydration energy (ΔG = -1080 kJ/mol) than Cl^- (ΔG = -340 kJ/mol) and NO_3^- (ΔG = -300 kJ/mol) making it more difficult to transport sulfate than a singly charged anion across a hydrophobic bilayer.[2] That Cl^- transport did not occur with intravesicular SO_4^{2-}, but was observed with a Cl^-/NO_3^- gradient, indicates that compounds **1b**, **4b** and **5** function by promoting anion exchange.

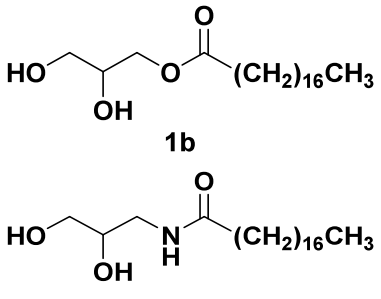

1b

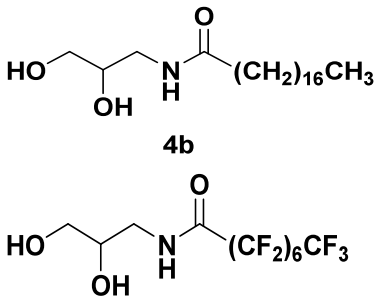

4b

5

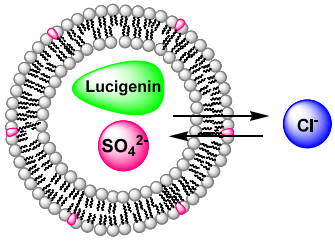

The Hill Equation. The Hill equation describes the relationship between the concentration of a substrate and an observed effect.[3] It has been often utilized in pharmacodynamics to describe the relationship between drug concentration (X) and observed drug effect (Y). A form of the Hill equation that is useful in the context of the supramolecular function of ion transport is shown below (equation 1), where K (EC_{50}) is the transporter's concentration for which 50% of maximum transport is obtained and n is the Hill coefficient of sigmoidality. The Hill coefficient has been interpreted to represent the molecularity of ligands required to mediate the observed effect.

$$Y = V_{max}.X^n / (K^n + X^n) \quad \text{(equation 1)}$$

The Hill equation can be applied to ion transport systems by examining the effect of varying the concentration of transporter [X] on the observed ion flux (Y). In this way, a value of K (EC_{50}) can be calculated and used to quantify transport activity- the lower the value of EC_{50}, the more potent is the transporter. Calculation of the Hill coefficient can provide mechanistic insight into the transport process, representing the number of transporter molecules required to transport a single ion; either as an aggregate mobile carrier complex, or as a self-assembled channel species.

To calculate the values of K and n for each compound, the transport assay was repeated for different concentrations of transporters that had been pre-incorporated into separate batchs of liposomes. The transport experiment was initiated by addition of an aliquot of aqueous NaCl (225 mM final concentration) at 25 ºC. The fluorescence of intravesicular lucigenin was monitored by excitation at 372 nm, and the emission was recorded at 503 nm with a 2.5 nm slit width. Thus, at t = 30 s, a 870 µL aliquot of a 1 M NaCl stock was injected to give a final NaCl concentration of 225 mM at 25 ºC. At the end of the experiment, 10 % aqueous Triton-X was injected to lyze the liposomes. This procedure describes how ion transport assays depicted in Figures S25-28 have been performed.

Lucigenin fluorescence was then converted to chloride concentration using the Stern-Volmer constant determined under the assay conditions. To measure the Stern-Volmer constant, liposomes were prepared as above, except that the liposomes were lysed immediately with Triton-X. Then, 5 µL of 4.0 M NaCl was titrated in every 30 s via the injection port. The titration was completed twice. A plot of f_0/f vs. chloride concentration was generated ($y=67.6x+1$, $R^2=0.9932$); the slope of which is taken to be the Stern-Volmer constant.

Using the Stern-Volmer constant and the lucigenin fluorescence data in Figures S24-27, the percentage of chloride anion that had entered into the vesicle at each transporter concentration was calculated at t= 270 s. The percentage of internal chloride vs. transporter's concentration was plotted and fitted to Hill equation 1. This enabled us to calculate values for K (EC_{50}), 270s, and for the Hill coefficient, n.

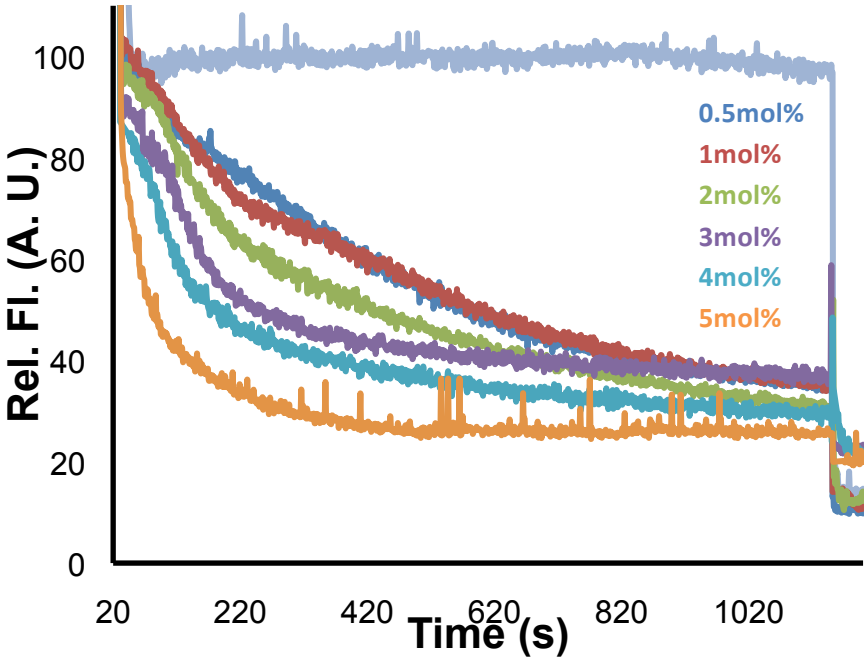

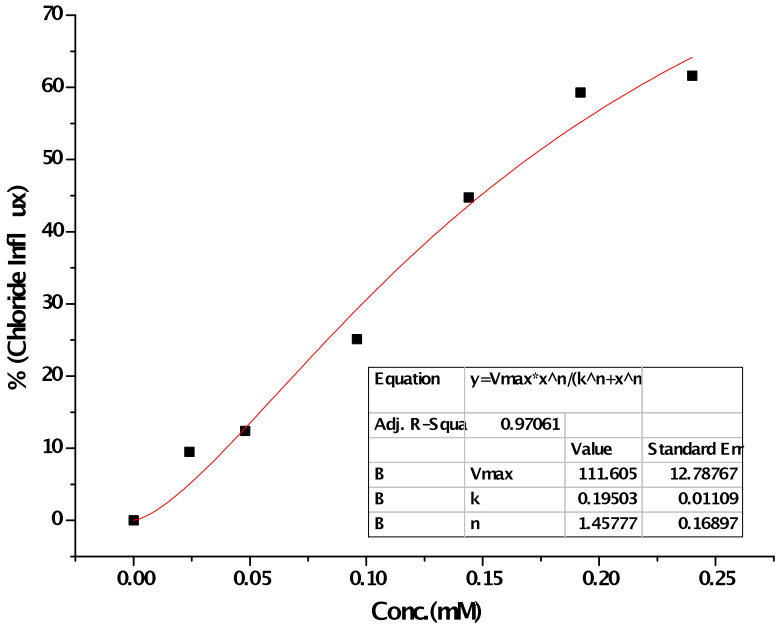

Figure S24. Using the Stern-Volmer constant and lucigenin fluorescence traces shown above, the percentage of chloride that had entered the liposome after 270 s vs. the concentration of monoacylglycerol **1a** was plotted and fitted to Hill equation 1. This enabled us to calculate values for K (EC_{50}), 270s, and Hill coefficient n. The relatively high EC_{50} values of compound **1a**, as compared to amide **4a** and perfluoro-amide **5**, reveals that the addition of the amide NH and fluorination of the acyl chain have a significant impact on transport efficiency in this systems. The perfluoro-amide **5** (0.011 mM) has an EC_{50} value that is almost 20-fold lower than the parent monoacylglycerol **1a** (0.195 mM).

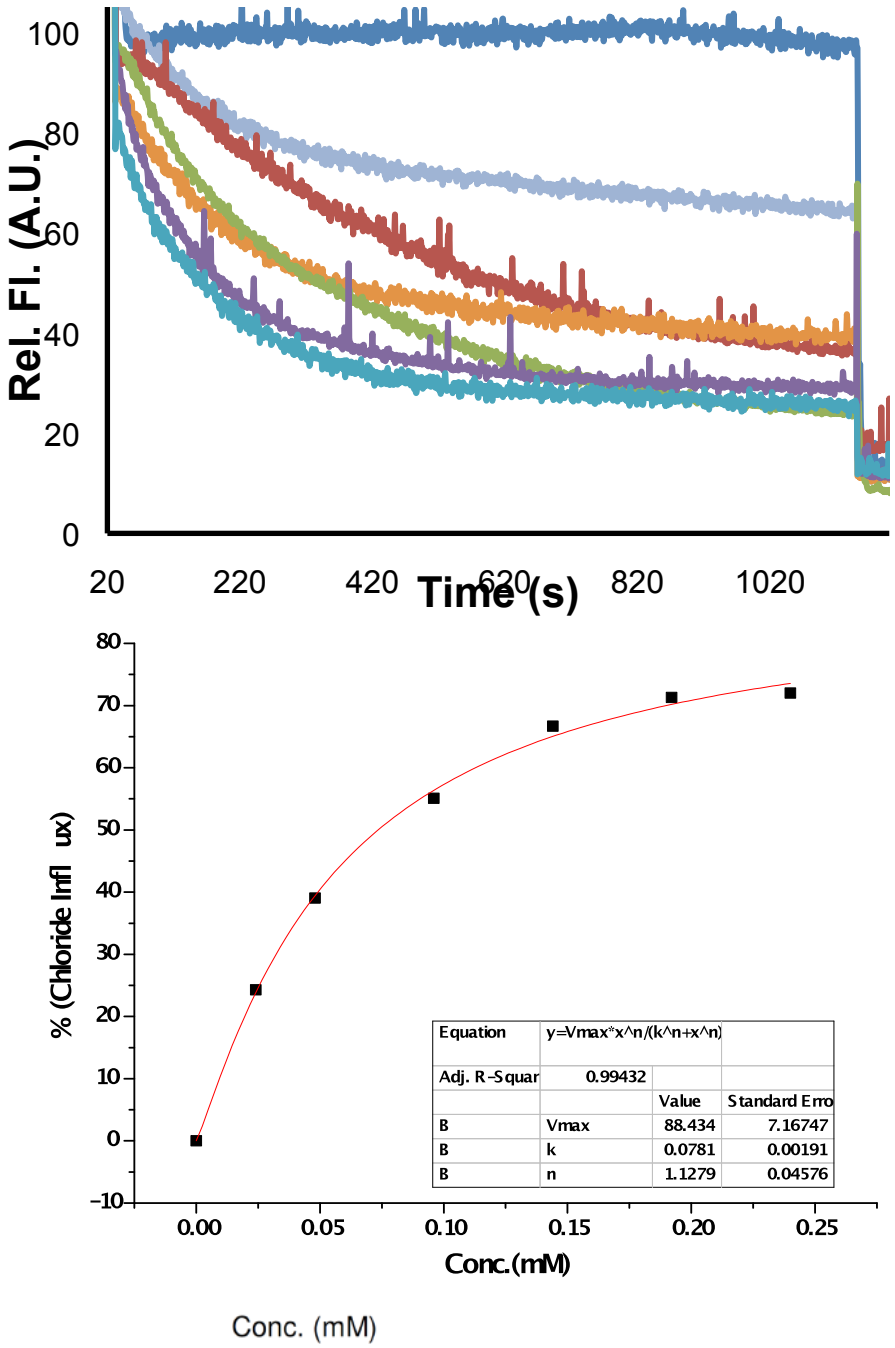

Figure S25. Using the Stern-Volmer constant and lucigenin fluorescence traces shown above, the percentage of chloride that had entered the liposome after 270 s vs. the concentration of amide analog **4a** was plotted and fitted to Hill equation 1 to calculate values for K (EC_{50}), 270s, and Hill coefficient n. Compound **1a** has higher EC_{50} value of 0.195 mM than **4a** (EC_{50} = 0.078 mM) which reveals that the addition of amide has a significant impact on the transport efficiency.

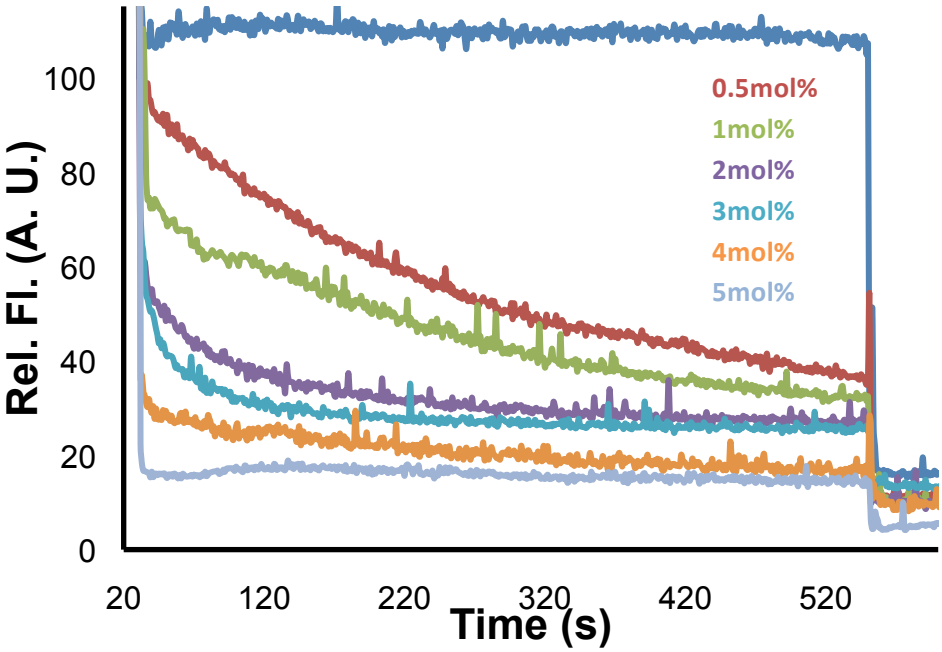

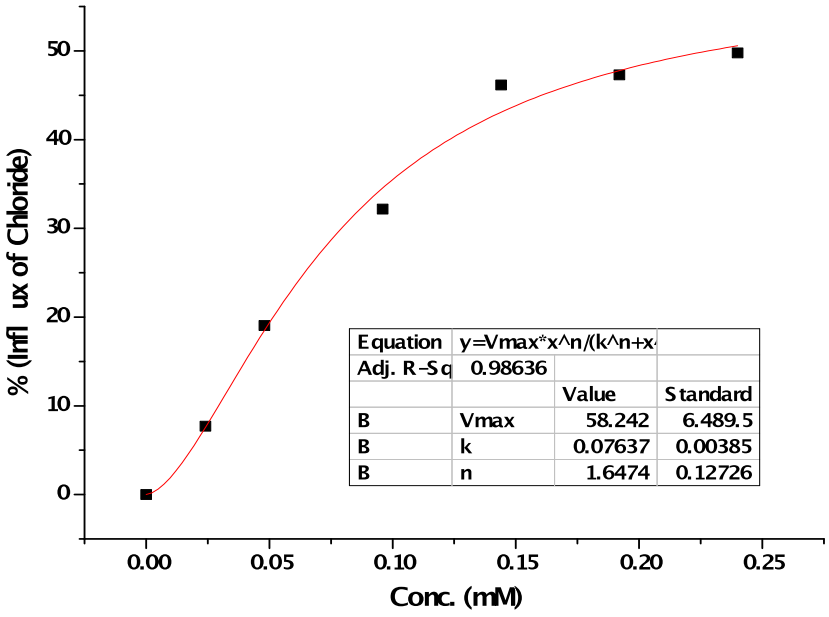

Figure S26. Using the Stern-Volmer constant and lucigenin fluorescence traces shown above, the percentage of chloride that had entered the liposome after 270 s vs. the concentration of amide analog **4b** was plotted and fitted to Hill equation 1 to calculate values for K (EC_{50}), 270s, and Hill coefficient n. The C18-amide **4b** has an EC_{50} value of 0.0764 mM while C8-amide analog **4a** has a modestly higher EC_{50} value of 0.0781 mM.

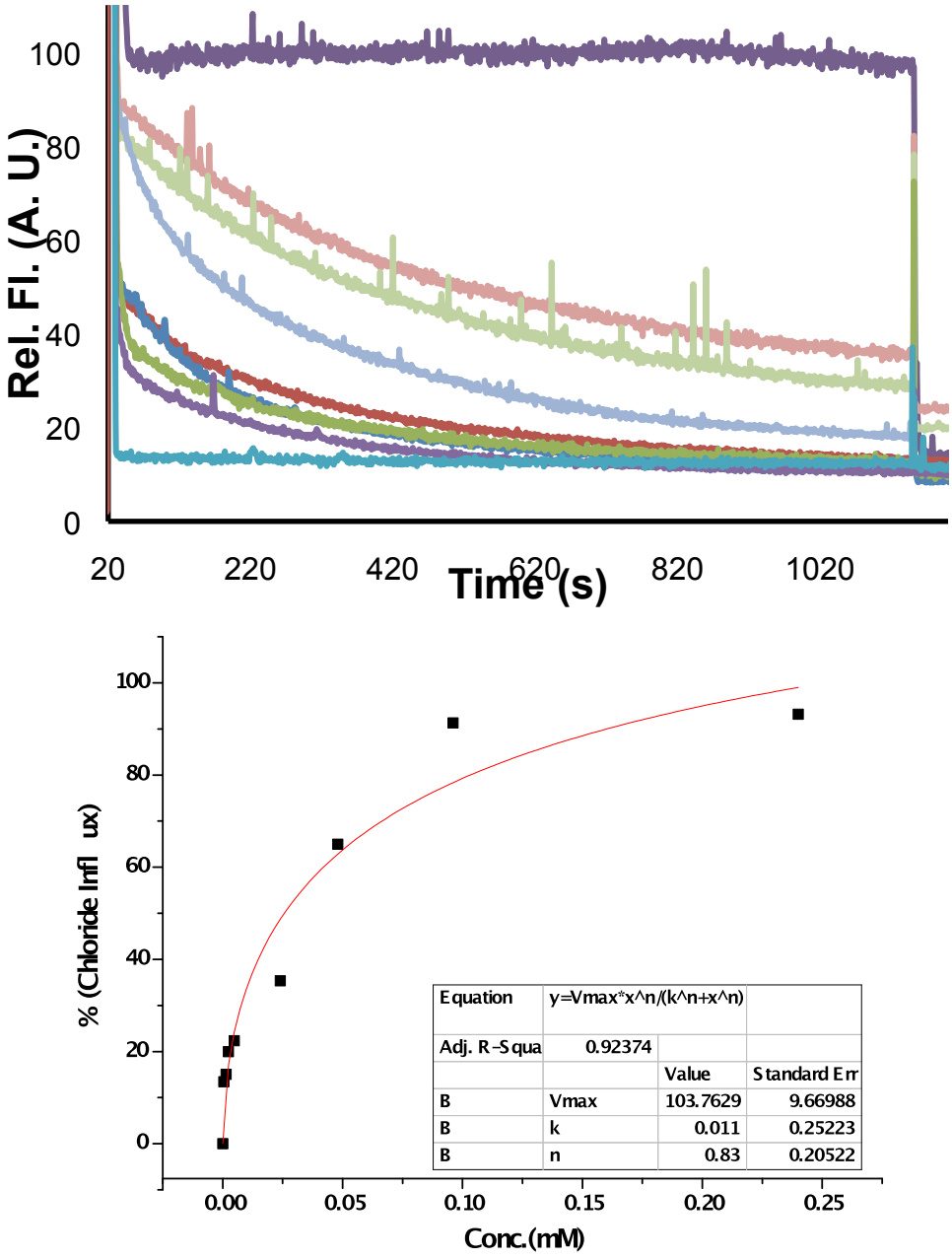

Figure S27. Using the Stern-Volmer constant and lucigenin fluorescence traces shown above, the percentage of chloride that had entered the liposome after 270 s vs. the concentration of perfluoro-amide **5** was plotted and fitted to Hill equation 1. This enabled us to calculate values for K (EC_{50}), 270s, and Hill coefficient n. The relatively low EC_{50} values for perfluoro-amide **5** reveals that both the addition of the amide NH and fluorination of the acyl chain have a significant impact on transport efficiency in this system, since **5** has an EC_{50} value (0.011 mM) that is almost 20-fold lower than the parent monoacylglycerol **1a** (0.195 mM).

Dynamic Light Characterization of Liposomes

The mean diameter, size distribution, and polydispersity index (PDI) of the liposomes were determined from measurements taken on a Photocor-FC dynamic light scattering (DLS) instrument. DLS measurements were made on 2 mL of a 0.4 mM solution of EYPC liposomes, containing 1 mol % of transporters **1a, 4a** or **5** and filled with HEPES buffer (20 mM, pH 7.4) and sodium nitrate (225 mM). An initial observation of the vesicle diameter was made (Table **S1**). Next, a pulse of 225 mM NaCl was added to the solution of liposomes. Any change in vesicle diameter after addition of the NaCl solution was noted. Liposomes were lysed using a 10% solution of Triton-X. Due to rupturing of vesicles by the detergent, no diameter readings were observed.

Table S1. Dynamic Light Scattering Characterization of Various Liposomes

Liposome	Size of polycarbonate membrane used (nm)	Measured diameter (nm)	
		EYPC	After addition of 225 mM NaCl
EYPC Blank*	100	106.7 ± 1.1	100.9 ± 1.2
Amide 4a	100	118.6 ± 1.2	105.9 ± 1.0
Perfluoro 5	100	112.2 ± 3.5	102.9 ± 0.9
Ester 1a	100	115.8 ± 6.2	103.8 ± 5.2

* Blank refers to EYPC liposomes that contain no added transporter.

Figure S28. Representative DLS data for EYPC liposomes containing 1 mol% of perfluorinated **5**:

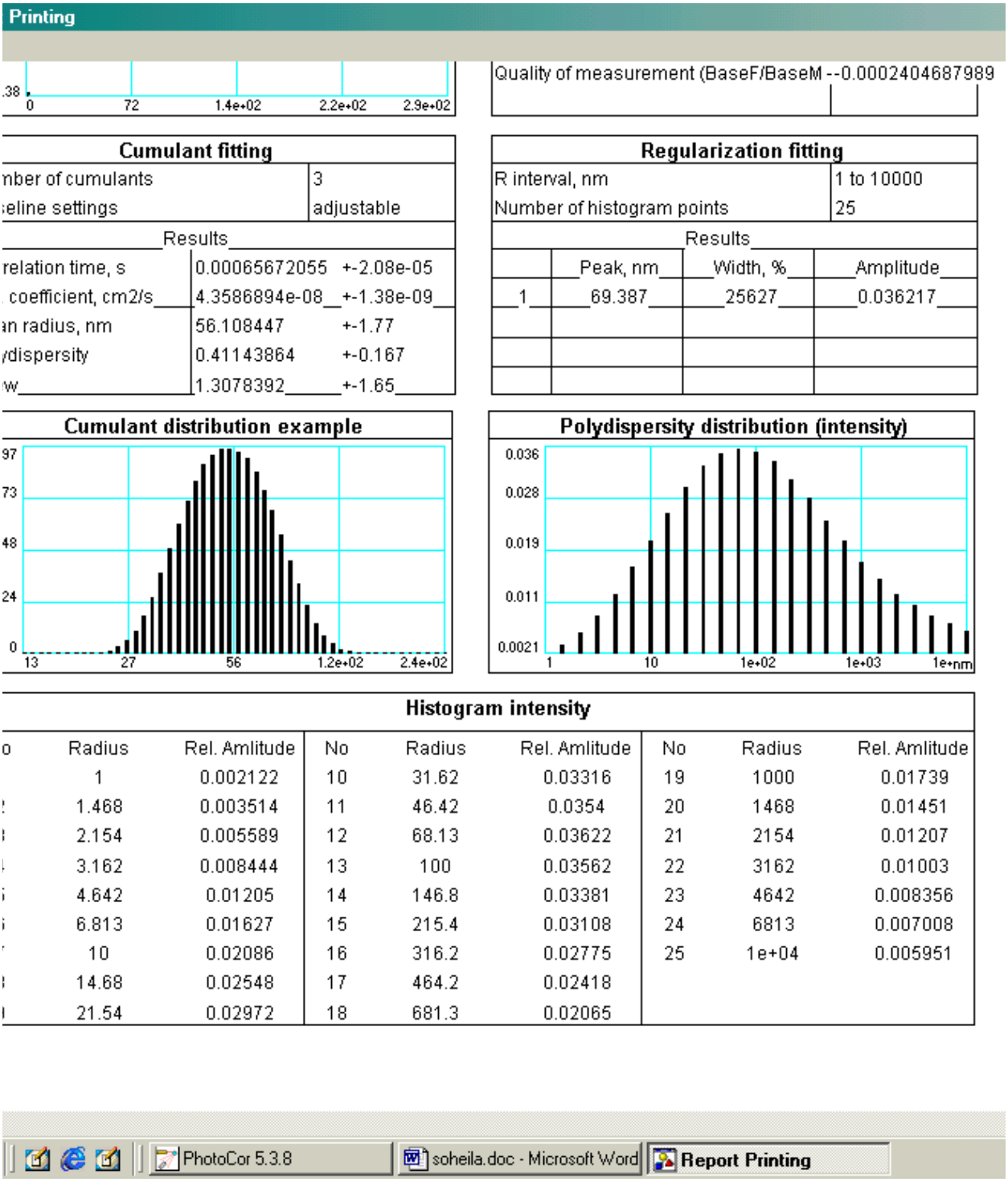

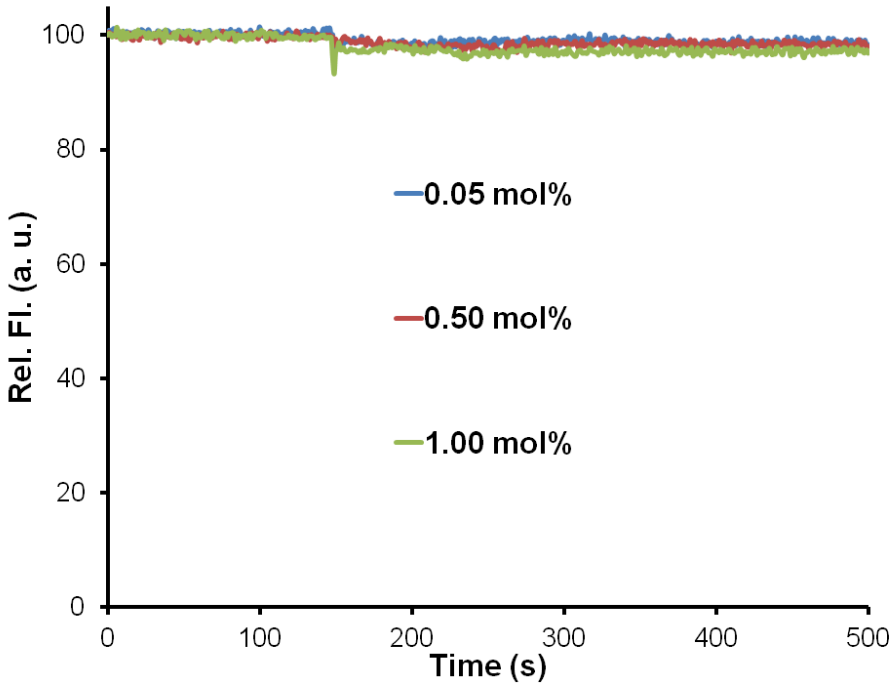

Figure S29. Control Experiment showing Influence of **5** on Lucigenin's Fluorescence. Aliquots of compound **5** were added to a solution of lucigenin (78 uM) in the absence of any EYPC lipid. The legend indicates mol % of 5 (assuming that there was the same amount of transporter as when 0.4 mM lipid was present); for 0.05 mol % (blue trace) the concentration of **5** was is 0.2 uM ii) for 0.5 mol % (red trace) the concentration of 5 was 2 uM and iii) for 1 mol % the concentration of **5** was 4 uM. It is clear that the monoacylglycerol analog **5**, itself, dose not quench lucigenin's fluorescence.

References

1. McNally, B. A.; Koulov, A. V.; Smith, B. D.; Joos, J. B.; Davis, A. P., *Chem. Commun.* **2005**, 1087-1089.

2. Marcus, Y., *J. Chem. Soc. Faraday Trans.* **1991**, *87* (18), 2995-2999.

3. Bhosale, S.; Matile, S., *Chirality* **2006**, *18* (10), 849-856.